CALCULATIONS FOR RF CAVITIES WITH DISSIPATIVE MATERIAL*

F. Marhauser#
Thomas Jefferson National Accelerator Facility, Newport News, VA 23606, U.S.A.

Abstract

For the design of RF devices like accelerating cavities, feeding and/or extracting RF energy requires antenna/waveguide ports, which present a perturbation to the otherwise closed system. Calculating Eigenmodes requires a numerical solver. The accurate numerical assessment and optimization of the external Q factors at such ports for a specifically excited RF mode or a mode ensemble can be crucial for proper operation of the device. Here a 3D Eigenmode solver technique is presented for the determination of the external Q, which makes use of dissipative material at external ports rather than the more traditional method of resembling matched conditions at external ports via the calculation of waveguide modes. This has advantages since both the external Q factor and the loaded frequency are calculated as part of the Eigenmode solver run (complex solution), while allowing for travelling mode conditions instead of standing waves. The technique does not require the external Q to be evaluated from subsequent runs with magnetically and electrically (closed) boundaries.

INTRODUCTION

With multi-processor and/or multithreaded processor systems becoming the norm, and increase in computer RAM capabilities as well as the improvement of numerical meshing options, comes the opportunity to incorporate complexities into numerical designs for realistic assessments on a reasonable timescale. This makes feasible studying subtle geometrical changes - which yet can have significant influence on the results - and detailed parametric studies allowing for fabrication tolerances. The latter becomes important when more stringent performance goals are imposed on RF devices - like accelerating cavities - that rely on conventional technologies, but make use of improved methods for production, surface treatments or the use of advanced materials to push operational limits to new frontiers.

The numerical determination of the external Q factor (Q_{ext}) has advanced over more than two decades from comparably tedious methods - when computational RF codes had no built-in capability to calculate Q_{ext} [1] - to very user-friendly codes with a 'one-click' option to compute Q_{ext}-values. This does not necessarily come though without significant expenses for commercially available software. Yet, the numerical simulations are often invaluable to meet scientific needs in order to turn a design into a properly operating device with a minimum effort of prototyping and thus development costs. The Q_{ext} calculation with dissipative material is elucidated in this paper by means of three relatively complex superconducting RF (SRF) cavities. For this purpose, capabilities of the frequency domain and Eigenmode solver of the CST Studio Suite [2] have been explored. The investigations has been triggered by software bugs in the CST Eigenmode solver that led to a false arrangement of mode numbers, principally due to sorting modes either in ascending order of the unloaded frequency (f_0) or the loaded frequency (f_l). Since the loaded frequency depends on the Q_{ext}, this can readily lead to ambiguous results, particularly when calculating of a large ensemble of Eigenmodes. The bug has been reported to CST at the time (CST version 2014). Using dissipative material (henceforth: absorber) instead of waveguide ports cured this problem, since the computed frequency is f_l. Furthermore, as part of Q_{ext} optimizations for fundamental power couplers (FPC) of SRF cavities (relatively high Q_{ext}-values), the results have been found to vary significantly depending on symmetry planes and/or the total number of modes used.

CALCULATION METHOD

Note that curved element tetrahedral meshes are employed throughout. This yields an accurate discretization of complex geometries. Each absorber placed in the domain can be optimized individually with respect to its reflection response (S11). Furthermore, each absorber can be placed arbitrary in the calculation domain to best resemble the real boundary conditions. At relatively high frequencies one or more propagating waveguide modes may participate in the external energy absorption depending on the excited Eigenmode in the structure. Waveguide mode conversion is also feasible as a cause of symmetry-breaking components. An advantage over the Q_{ext} determination with waveguide ports is that one does not need to predefine the number of traveling modes for absorption (with unconsidered modes reflected at the boundary, but more modes increasing the calculation time), nor does an external port has to end with a planar boundary. Additionally, waveguide modes are calculated at a center frequency given by the frequency range. This can elevate inaccuracies of matched conditions when a cutoff frequency is present, i.e. the further the Eigenfrequency is apart from the center frequency. The presented method instead can account for

* Authored by Jefferson Science Associates, LLC under U.S. DOE Contract No. DE-AC05-06OR23177. The U.S. Government retains a non-exclusive, paid-up, irrevocable, world-wide license to publish or reproduce this manuscript for U.S. Government purposes.
# marhause@jlab.org

well-matched absorbers over a wide frequency range. Moreover, it can resemble the finite reflection of a realistic absorber. For the latter a dispersion list can be used based on complex dielectric and/or magnetic material properties that are measurable.

Frequency Domain Solver

Prior to the Eigenmode solver run, the complex material properties and the shape of the absorber is optimized in frequency domain to fulfill certain reflection response criteria. These calculations are rather effort-less since the absorber can be located at the end of a relatively short waveguide based on the cross-section of the specific external port. This limits the number of mesh cells and computation time. The relative permittivity and/or permeability and the corresponding loss tangents as well as geometrical parameters can be chosen as free parameters to converge to the desired performance goals over a wide frequency range. The use of the implemented optimizer in CST is recommended. This allows setting target requirements for S11 as well as margins for the parameters such that no further user intervention might be necessary to yield satisfying results with a single optimization run. For RF cavities, waveguide ports are employed that may intersect with resonant cells or beam tubes. The cross-sections are typically rectangular or round with or without ridges or shaped like a dog bone to minimize the magnetic flux density at cavity/port intersections. In all cases, a broadband match can be achieved with rather simple wedged-shaped absorbers, i.e. tapered to yield a smooth impedance transition for the respective waveguide mode. For coaxial coupler ports, the space between the inner and outer conductor may be filled completely with absorptive material to provide a broadband match.

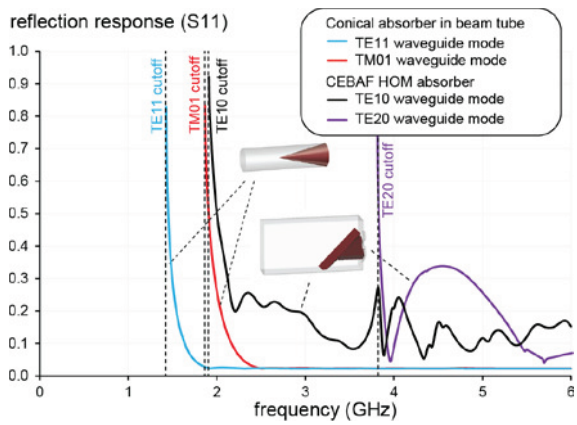

Figure 1: Reflection response (linear scale) for two absorber shapes as calculated in frequency domain.

Figure 1 exemplarily shows the S11 for a conical absorber in a round tube and for an absorber in a rectangular waveguide. The latter represents the Higher Order Mode (HOM) loads employed in original CEBAF SRF cavities (cf. Fig. 6 further below). For the conical absorber, the material parameters are artificial and optimized to result in almost a 100% RF absorption up to 6 GHz above the waveguide cutoff frequency. As shown, this is true for both the TE11 and TM01 waveguide mode with the absorption decaying swiftly above the respective cutoff frequency. The CEBAF absorber is a lossy ceramic working at 2 Kelvin. The material data were provided as a dispersion list based on measurements resulting in realistic S11 parameters [3]. Here the S11 for the TE10 (~1.9 GHz cutoff) and TE20 waveguide mode (~3.8 GHz cutoff) are depicted.

Eigenmode Solver

Once an absorber is optimized, it can be reemployed in the Eigenmode solver as part of the full RF structure. For SRF cavities the wall losses are usually negligible compared to the external losses ($Q_{ext} \sim Q_l$). Otherwise the loaded Q is computed. Consequently, to account for the external Q only, the default conductivity (copper) of the conducting enclosure should be changed to a perfect electrical conductor (PEC). This means that all losses are attributed solely to the absorbers placed in the external ports. Two options are available to determine the external Q. One is based on the usual perturbation method (henceforth: $Q_{ext,pert}$). Note that in cavities without dissipative material, this perturbation method yields the unloaded Q_0 given the surface conductivity of materials. Here it account accounts for both the surface losses (zero for PEC) and the volume losses in the absorber(s). The second method calculates the Q_{ext}-value based on the complex Eigenfrequency of the lossy Eigenmode (henceforth: $Q_{ext,lossy}$). The complex Eigenfrequency arises since energy can be absorbed externally, which changes the frequency compared to that of a closed system as already mentioned above. The shift of the frequency due to external damping results in an imaginary part. The frequency calculated then corresponds to the loaded frequency. If $f_0 \approx f_l$ (for Q_{ext}-values on the order of 1e7 or higher) it has been noted that $Q_{ext,lossy}$-values are typically denoted as zeros, while $Q_{ext,pert}$ still provides finite numbers.

EXAMPLE A - TESLA/XFEL/LCLS-II NINE-CELL CAVITY

The well-known TESLA-type 1.3 GHz nine-cell cavity [4] is employed at multiple laboratories worldwide, most prominently at the Free Electron Laser Facility at DESY in Hamburg/Germany (FLASH) and the European XFEL facility (under construction). The RF cavity design (see Fig. 2) has also been chosen for the proposed Linac Coherent Light Source (LCLS)-II and conceived for the future International Linear Collider (ILC) project. The cavity accommodates two HOM hook antennas ('F-parts') housed in round cans attached to the beam tubes located close to the end cells (cf. Fig. 3). The beam-induced, parasitic HOM energy is extracted via coaxial RF vacuum feedthroughs coupling capacitively to the F-part. The energy is then transferred by cables away from the cryogenic environment to terminate in standard 50 Ω loads at room temperature.

ISBN 978-3-95450-178-6

The XFEL feedthrough differs from that of the original TESLA-cavities, particularly with regard to the probe tip shape as depicted in Fig. 3. The XFEL-style feedthrough has been adapted for LCLS-II, i.e. CW operation by conceiving proper conduction cooling. Hereby, it is important to keep the Niobium probe superconducting. For tetrahedral meshing has been locally refined for both HOM end-groups to allow for well discretized F-parts and probe tips and account well for the capacitive gap between the probe tip and the planar side of F-part

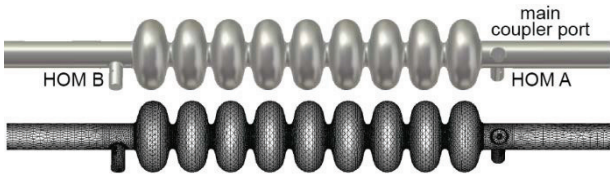

Figure 2: TESLA cavity model (top) and its tetrahedral mesh representation using CST (bottom). Here comparably long beam tubes are used on each side to incorporate conical absorbers (not shown).

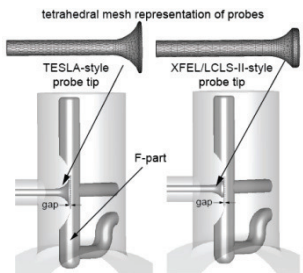

Figure 3: TESLA-style vs. XFEL-style probe tip design.

The Q_{ext}-values have been calculated by terminating the coaxial ports of both HOM couplers with absorbers. Results are shown for the first (TE111) and second dipole (TM110) passband in Fig. 4. The beam tubes and main coupler port have also been terminated. This does not play an important role for first two dipole passbands since modes resonate below the TE_{11} beam tube cutoff frequency. The results for both $Q_{ext,pert}$ (black dots) and $Q_{ext,lossy}$ (blue triangles) are comparable yielding Q_{ext}-values below 1e6 throughout. The horizontal polarized modes are typically better damped than the vertically polarized dipole modes due to the azimuthal configuration of the HOM couplers. Experimental results are shown in comparison. These have been carried for two LCLS-II cavities dedicated for use in the first LCLS-II prototype cryomodule assembled at JLab. The cavities (welded to helium tanks) have been tested in JLab's horizontal test cryomodule (AES033, red diamonds) and in the vertical test stand (AES036, green diamonds) at cryogenic temperatures. The simulations are in well agreement with measurement data confirming the accuracy when using dissipative loads. Note that the measured data for both cavities already reveal deviations that are partly larger than those experienced between $Q_{ext,pert}$ and $Q_{ext,lossy}$ for similar type of passband modes. This is due to fabrication tolerances, e.g. variations in deep-drawing of cells, trimming, tuning and other post-processing procedures like differing interior surface removal by chemistry.

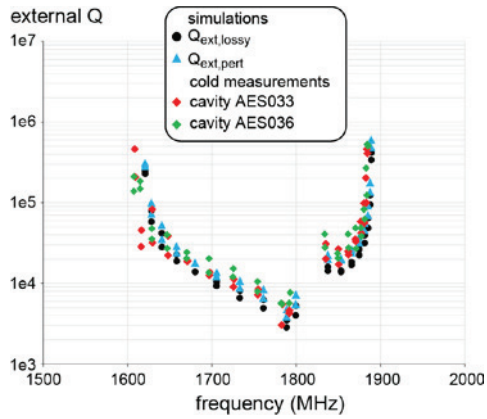

Figure 4: Q_{ext}-values of TE111 and TM110 passband modes in the TESLA-cavity using XFEL-style RF probe tips as simulated and measured.

Simulations can show discrepancies to measured data for same reasons, since the numerical model typically cannot account for all fabrication-related geometrical deviations, though differences are comparably small in the study above. Yet, subtle deviations can change results significantly. This can be examined numerically to evaluate the impact of fabrication tolerances as done in Fig. 5. Herein Q_{ext}-values are calculated for the same modes shown in Fig. 4, but in dependence of the gap width between the probe tip and the F-part varied from 0 to 0.5 mm in steps of 100 µm (for both couplers).

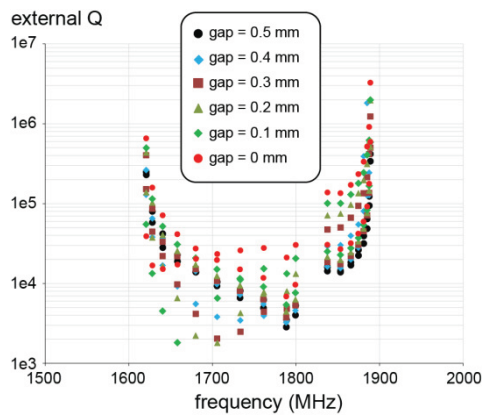

Figure 5: Simulated Q_{ext}-values (here $Q_{ext,lossy}$ only) of TE111 and TM110 passband modes as in Figure 5, but in dependence of the gap width between the probe tip and the F-part as noted in the legend (changed for both HOM couplers simultaneously).

Overall, shortening the gap is least favourable for these dipole modes. The nominal gap width is 0.5 mm (as assumed for Fig. 4). With subtle deviations of this dimension alone, a comparably large deviation in the Q_{ext}-values can be expected. Note that the gap width is tolerated with +0.2/-0.1 mm for XFEL cavities [5].

The tables below exemplarily summarize results for a small ensemble of modes computed either terminating the HOM couplers and FPC with absorbers (Table 1) or with waveguide ports (Table 2). The latter technique yielded a factor ~1.8 longer solver time in this case. It also resulted in f_l and Q_{ext} being identical for the first two modes, though the unloaded frequency and vector fields accounted for all three different modes (CST Studio Suite 2015, SP4). The Q_{ext}-values of the modes are overall significantly different compared to $Q_{ext,lossy}$ and $Q_{ext,pert}$.

Table 1: LCLS-II Cavity Using Absorbers (446220 Mesh Cells, Solver Time = 1 hr 13 min)

Mode #	f_l MHz	$Q_{ext,\ pert}$	$Q_{ext,\ lossy}$
1	1788.492	9.45e3	6.88e3
2	1789.043	2.90e4	2.11e4
3	1799.454	1.33e4	9.65e3

Table 2: LCLS-II Cavity Using Waveguide Ports (435658 Mesh Cells, Solver Time = 2 hrs 12 min)

Mode #	f_0 MHz	f_l MHz	Q_{ext}
1	1788.931	1789.189 (?)	4.44e4 (?)
2	1789.118	1788.189 (?)	4.44e4 (?)
3	1799.756	1799.952	5.76e4 (?)

EXAMPLE B - CEBAF ORIGINAL FIVE-CELL CAVITY

The updated 12 GeV CEBAF electron recirculator still relies in majority on the original 1497 MHz five-cell SRF cavities using the HOM absorbers described above. For Q_{ext} studies using absorbers instead of waveguide modes, the RF model has been equipped with the absorbers based on measured material properties (cf. Fig. 1) and with or without a broadband load placed in the rectangular fundamental power coupler (FPC).

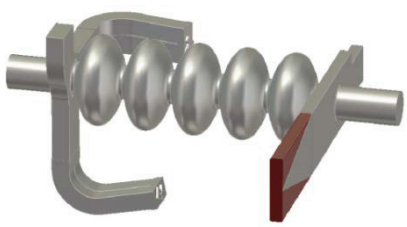

Figure 6: Five-cell original CEBAF SRF cavity with realistic absorbers (not visible) placed in each of the two HOM waveguides (left side of cavity) and a broadband absorber in the FPC (right side of cavity).

The findings are plotted in Fig. 7 for the first two dipole passbands residing below the TE11 beam tube cutoff frequency such that the boundary conditions at beam tubes are negligible. It reveals that a few TE111 mode pairs are also located below the TE11 cutoff frequency (~1.9 GHz) of the HOM waveguides.

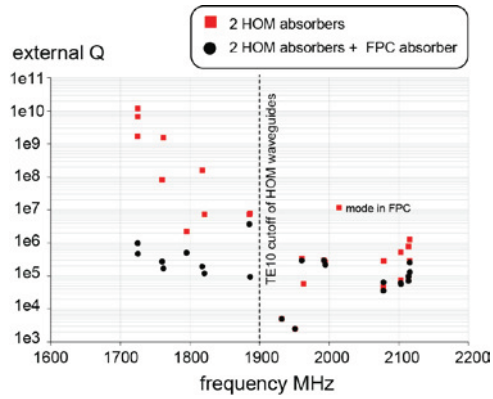

Figure 7: Simulated Q_{ext}-values (here $Q_{ext,lossy}$ only) of TE111 and TM110 passband modes in the original CEBAF cavity.

Without utilizing an FPC absorber, the Q_{ext}-values of some TE111 modes would be as high as 1e10 yielding high impedances, i.e. a concern for beam break-up instabilities. Once an absorber is placed in the FPC waveguide (TE10 cutoff is ~1.1 GHz), the values are reduced by several orders of magnitude thanks to damping via the FPC waveguide. Note that the FPC points in horizontal direction. The Eigenmode solver revealed though that both polarizations of the TE111 modes may couple to the TE10 mode, though with different strength. The damping via the FPC was well considered at CEBAF in the past. Therefore, each FPC waveguide is equipped with a special HOM filter external to the cryomodule, which is designed to let through the incoming wave from a generator with high efficiency.

Using dissipative material in the simulation allows investigating the traveling field in the coupler under matched conditions.

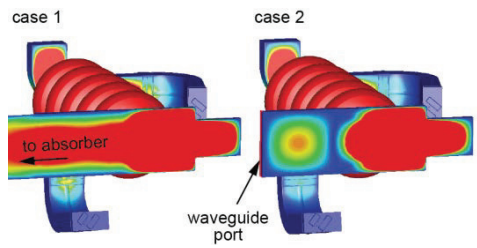

Figure 8: Contour plot of the average electrical field of the accelerating mode implying a traveling mode for the case of an absorber placed inside the FPC (left) and a standing mode in the FPC when a waveguide port (right).

The contour plots in Figure 8 for instance reveal the average electrical RF field for the accelerating TM010 mode in the FPC for the case when the FPC waveguide is matched with an absorber (left) compared to the case when a waveguide port has been used. The contours imply a traveling mode for the first case, and a standing mode pattern for the latter. The stub at the end of the FPC waveguide will reflect the incoming mode and can be optimized with respect to coupler kicks, i.e. the deflection of a main beam caused by the accelerating mode.

ISBN 978-3-95450-178-6

EXAMPLE C - DOUBLE QUARTER WAVE CRAB CAVITY

An SRF Double Quarter Wave Crab Cavity (DQWCC) has been designed as a potential candidate for the Large Hadron Collider (LHC) high luminosity project [6]. It aims to employ the crab-crossing technique to increase the luminosity of colliding beams in favour of providing more beam energy. The crabbing mode resonates at the lowest frequency of 400 MHz and has to provide a deflecting voltage of 3.34 MV. Parasitic HOMs must be damped sufficiently. The DQWCC thus incorporates three rather complex HOM filters. A detailed HOM analysis has already been done elsewhere using the waveguide port technique [6]. E.g. for risk mitigation, extensive calculations were performed to understand the impact of fabrication tolerances on HOM damping, particularly related to coupler geometrical details. Here an RF model of the DQWCC design has been set up as shown in Fig. 9 to compare findings, when utilizing absorbers (case 1) versus waveguide ports (case 2).

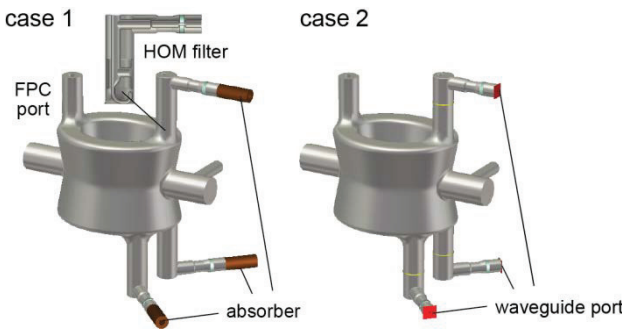

Figure 9: DQWCC model prepared for Q_{ext} calculations with absorbers (case 1) or waveguide ports (case 2).

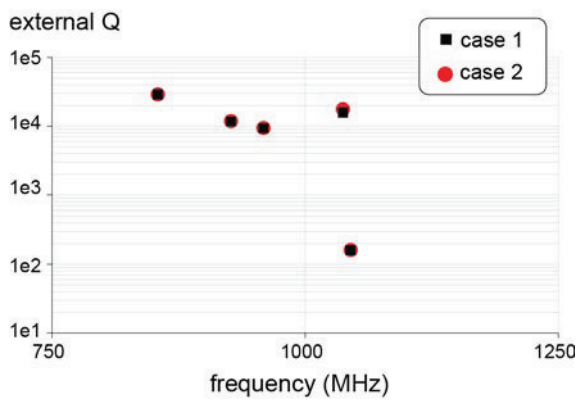

Figure 10: Simulated Q_{ext}-values (here $Q_{ext,lossy}$ for case 1) of several HOMs in the 400 MHz DQWCC crab cavity.

Only a few Q_{ext}-values were calculated for this study. Figure 10 reveals that both techniques delivered results in well agreement and for HOMs with $a_{ext}Q < 1e5$ in contrast to the example B.

SUMMARY

A technique for external Q calculations using CST Design Studio has been described employing dissipative material as absorbers. The absorbers can be optimized as broadband loads or with a realistic reflection response characteristic. This has shown to provide reliable results based on comparisons with experimental data and with findings for the more traditional method that utilizes waveguide ports to resemble matched conditions. The latter method though has been found to deliver doubtful results in some cases. Moreover, a software bug has been identified with regard to sorting mode numbers, which can cause ambiguities without careful revision (current CST version). The Eigenmode solver might not always converge swiftly (for both techniques). It is recommended that the calculation with absorbers is carried out sequentially for a rather small number of modes (4-10). In most cases the computational time then decreased when compared to the waveguide mode technique, though sometimes a slow convergence has been observed depending on the specific modes. E.g., computations using a standalone two-processor workstation (Intel Xeon CPU E5-2670 v3, 128 GB RAM) required a few working days to compute all crucial HOMs up to 3.2 GHz in the fully 3D LCLS-II cavity with refined HOM coupler discretization (300-450 curved surface tetrahedral mesh cells). The sequential computations can be automatized with CST. The user-dependent post-processing analyses require separate solver time. E.g. R/Q-values can be computed at any offset from the beam axis if desired, which together with the Q_l (~Q_{ext} for SRF cavities) yields the shunt impedance of longitudinal and transverse modes. In this respect and for high-Q modes present, Eigenmode calculations can be significantly faster than deriving impedances from long-range wakefield calculations. In each case, inaccuracies usually rise with an increase of the Q_{ext}-value. Differences in results between $Q_{ext,lossy}$ and $Q_{ext,pert}$ are further scrutinized.

ACKNOWLEDGMENT

The author likes to thank Mircea Stirbet from JLab for providing the HOM measurement data for the LCLS-II prototype cavities and Binping Xiao from BNL for providing the DQWCC RF model for analysis.

REFERENCES

[1] N.M. Kroll, D.Y.L. Lu, SLAC-PUB-5171.
[2] https://www.cst.com
[3] I. Campisi et al., Proceedings of 6th Workshop on RF Superconductivity, Newport News, VA, USA.
[4] B. Aune et al., Physical Review Special Topics-Accelerators and Beams **3**, 092001 (2000).
[5] J. Iversen, DESY, private communication.
[6] B. Xiao et al., WEPEI059, Proc. IPAC 2015, http://jacow.org/